Analysis of the thermal efficiency of a compound parabolic Integrated Collector Storage solar water heater in Kerman, Iran

Rashid Panahi [1], Mohammad Hassan Khanjanpour [2], Akbar A. Javadi [2], Mohammad Akrami [2], Mohammad Rahnama [1], Mehran Ameri [1]

[1] Department of Mechanical Engineering, Shahid Bahonar University of Kerman, Kerman, Iran

[2] Department of Engineering, College of Engineering, Mathematics, and Physical Sciences, University of Exeter, Exeter, United Kingdom

*Corresponding authors

*Akbar A. Javadi,

Harrison building, North Park Road, College of Engineering and Physical Sciences, University of Exeter, EX4 4QF,

Phone: 01392723640,

A.A.Javadi@exeter.ac.uk

Keywords: Solar water heater; Integrated Collector Storage; Compound parabolic concentrators; Thermal performance; Sustainable development

Abstract

This paper presents an experimental study involving design, manufacturing and testing of a prototype integrated collector storage (ICS) solar water heater (SWH) in combination with a compound parabolic concentrator (CPC). The thermal efficiency of the developed system is evaluated in Kerman (latitude 30.2907°N, longitude 57.0679°E), Iran. A 6-month experimental study was undertaken to investigate the performance of the ICS SWH system. The mean daily efficiency and overnight thermal loss coefficient of each experiment were analyzed to examine the appropriateness of these collectors for regions in Kerman. The results showed that mirror has the highest mean daily efficiency (66.7%), followed by steel sheet (47.6%) and aluminium foil (43.7%). The analysis of hourly and monthly operation diagrams for variations of water temperature for the developed system showed that by increasing the amount of radiation entering the water heater, the system's thermal efficiency decreases, such that the highest efficiency (during the six-month test period) was in April (66%) and the lowest in July (50%). The study shows how the temperature gradient between the ambient air and internal water in the storage tank can influence the performance of such systems, and how a controlled amount of hot water withdrawal can affect the system's efficiency.

Introduction

Industrialization and population growth have caused a dramatic rise in the annual consumption of fossil fuels [1]. Since 1859, most everyday energy usage relied directly or indirectly on fossil fuels. This has caused many environmental problems such as global warming, acid rain, water pollution and increased waste and environmental degradation. By implementing new technologies based on utilizing renewable energy sources, the reliance on fossil fuels dwindles, and the contamination casused by them can also be reduced. Planning and developing new energy sources to replace fossil fuels has increased over the past two decades [2] to be used for different applications [3-6]. Solar energy is one of the more reliable sources of renewable energy and can provide 173,000 TW of energy daily to the earth [7]. Although the amount of solar energy that reaches the ground is abundant, its rate per unit area is low. A major challenge is therefore to collect and concentrate this energy efficiently, which is usually done using solar water heaters.

Solar water heaters can be divided into two main categories: active and passive systems [8, 9]. The active system consists of a solar collector to absorb solar energy and a tank for storing hot water. It includes three main types: direct, indirect, and drain back. In the direct systems, the water circulates directly to the collector. When the temperature of the collector is greater than that of the tank, a pump will circulate the water from the source to the collector. These systems are generally not recommended for climate conditions that lead to cooling of the system or in cases that use heavy or acidic water [10].

The indirect systems use antifreeze fluids such as propylene glycol in the collector for the purpose of transferring the heat. The low freezing point of propylene glycol prevents the freezing of the system and allows the solar systems to be used under conditions below 0 ^{o}C. The indirect systems prevent the reverse flow of thermosiphon by using a one-way valve at night [11]. The third type of active system is the water-back system. Water-back systems use water for heat transfer. To prevent the risk of frost when the collector temperature is lower than the tank temperature, the pump is switched off and the water inside the system returns to the reserve. The space inside the collector is then filled with air, which protects against the freezing of the system [12].

Although active systems are relatively easy to set up, efficient passive systems are also utilized based on their own capabilities. These are divided into two systems: Thermosiphon and ICS. The Thermosiphon system uses high radiation absorption when it is heated (decreasing density). In this system, a storage tank is installed at an altitude higher than the collector. When the water is heated, it becomes lighter and naturally flows to the highest point inside the supply. The cold water from the bottom of the source flows through the pipes to the bottom of the collector and creates a natural circulation in the system. Circulation in the system stops when the temperature inside the collector becomes lower than the temperature inside the tank. This prevents heat transfer from the system to the environment at night when the temperature of the collector is lower than that of the supply [13]. In the ICS type of passive SWHs, the storage tank and the collector are not separated from each other. The cold water is directly connected to the collector and is heated by the sun. Unlike other systems, hot water remains in the collector until it is consumed and then directly used by the collector. ICS systems require larger storage sources (to increase radiation absorption capacity) than conventional systems, which also protect the system against frost [14].

Many amendments have been made in recent years to various parts of the ICS system so that the maximum absorption of radiation energy and the lowest thermal loss can be achieved simultaneously for the system. From the early 1800s, a number of solar concentrators were built to achieve higher temperatures and steam production [15]. The first ICS SWH was developed in the southwest of the USA at the end of the 18th century. In 1982, Tiller and Wochatz analyzed the performance of ICS water heaters in warm climates and discovered that ICS' performance is higher than flat plate SWHs [16]. In another experimental study, a solar water heater (SWH) with a plastic water bag (PWB) was designed and developed that produced desirable results in different weather conditions [17]. In 1984, Faiman provided a standard method for calculating the efficiency of ICS SWH water heaters [18]. This methodology helped Waller et al. [19] to analyze the rate of heat loss in ICS solar water heaters. Rommel [20] concluded that transparent insulating materials can increase the efficiency of ICS water heaters. Mohammed et al. [21] constructed an ICS SWH with a buffer inside a repository, which showed better efficiency in comparison to non-buffer SWHs. Tripanagnostopoulos & Souliotis [22] designed four different models with asymmetric geometries by analyzing the system's heat loss during the night and their thermal performance. The results were compared with the CPC concentrator. It was shown that the SWH with asymmetric geometry had less thermal dissipation at night than the SWH with symmetrical geometry, and the system with symmetric geometry had a higher efficiency than the others [22].

Regional studies were also planned to provide a database for governments and decision makers to invest their budget wisely. One of these studies examined the resistance of a water heater to frost in northern European climate conditions [23] to establish an economic evaluation of ICS water heaters in mass production. In this study, the researchers analyzed the return on investment (ROI) and showed that a large number of ICS water heaters was economical and also technically feasible [24]. In 2003, Souliotis & Tripanagnostopoulos [25] conducted experiments on various ICS solar water heaters. They constructed three water heaters with different CPM profiles with different dams and showed that the SWH with a 30-cm droplet dryer had better thermal performance. In another study, the temperature classification of ICS water heaters with a horizontal storage tanks was experimentally evaluated to investigate the effects of multiple combinations of such systems

[26]. In 2008, Souliotis and Tripanagnostopoulos [27] analyzed the general distribution of water in the tank wall of the heater. The results illustrated that the upper part of the source reserve absorbed the majority of the reflected radiation. The first study on optical performance of an ICS heater was published in 2015 [28]. The results of this study provided a significant improvement in optical efficiency and the distribution of radiation absorption with various solar slope angles. In the following year, the same researchers optimized the geometrical characteristics of an ICS SWH system in order to find the optimal thermal performances [29]. Most recently, Harmim et al. [30] simulated and tested an ICS SWH for integration into a building façade. Their system had a daily efficiency between 36.4 and 51.6% and its thermal loss coefficient during night-time was between 2.17 and 3.12W. The results from these studies showed that different regions receive different amounts of energy based on their assigned latitudes.

Because of their location, some countries have benefited from a greater amount of solar intensity [31]. One of these countries is Iran, which is located at a latitude of between 25 to 40 degrees North. The amount of solar radiation in Iran is estimated to be between 1800 and 2200 kWh/m^2 per year, which is higher than the global average [32]. In Iran, on average more than 280 days per year are sunny, which is higher than a vast majority of the countries within Europe [33]. Therefore, it can rely on different forms of solar energy solution to generate electricity and provide the heating requirements for residential homes. By analyzing all sites of Iran, Shiraz, Yazd and Kerman have areas with higher solar radiation, as illustrated in the solar GIS map [34]. Unfortunately, due to the fact that Iran has one of the largest endowment of oil and natural gas resources in the world [35], most of the population of these regions are already utilizing natural gas for heating water [36]. In this regional study, the Kerman Province, which has 23 cities and encompasses more than 11% of Iran's terrestrial area, was selected for investigation [37]. In addition, its vicinity to the Lut Desert, lower population density and abundance of remote villages compared to its neighboring provinces are other features making it apt for investigating solar water heaters [38]. Although the technologies to generate electricity such as photovoltaic (PV) systems have started to be used in Iran, the applications of solar water heaters has received little to no attention. This technology can be widely used to provide hot water for domestic and industrial consumers in Kerman province, as well as other regions around the world with similar conditions that have considerable solar radiance (see Fig. 1) [39].

The system presented in this paper has several advantages: it is economically affordable, structurally robust and easy to manufacture and install using local material, especially in developing countries. Although there have been some studies on ICS SWH systems in some parts of the world, the findings cannot be easily extended to other specific regions. Furthermore, long-term experiments on the performance and efficiency of ICS SWH systems is rare in the literature. In the following sections, the design and testing processes for an ICS SWH system for Kerman Province is presented and discussed.

2. Geometric design of the ICS SWH system

2.1. Storage tank

The storage tank is the central part of the ICS SWH system. Its function is to absorb solar radiation and transfer the thermal energy to the stored water. The size and shape of a storage tank have an important effect on the absorption of solar energy. The greater the area of the storage tank exposed to the sun, the less time it takes to warm the water. However, in a normal climate, a high-surface storage tank will lose a significant part of the energy through heat transfer and radiation with long wavelengths, and mostly during the night due to heat loss to the surroundings [40]. According to the study carried out by Keshavarzia et al. [41], water consumption in rural regions of Iran is about 120 l/d per person. In order to supply this amount of household water, the diameter and length of the storage tank were chosen as 30 cm and 200 cm respectively, resulting in a storage tank volume of just over 141 l. The storage tank should be made of high conductivity material such as aluminum, copper or galvanized iron/steel [42]. The thickness of the sheet should be chosen such that it withstands the pressure of the water, in addition to having low thermal resistance against heat transfer [40]. Considering the available sheets in the market, a thickness of 1 mm was chosen.

2.2. Geometry of CPC concentrator

A symmetric CPC concentrator was selected to achieve the highest efficiency based on literature [22] (see Fig. 2).

Fig. 2 - Cross-section view of a symmetric CPC [22]

In such models, the concentrator is composed of four parts: AB, BC, C'D, and DA' (see Fig. 2). The parabolic equations for the different parts are as follows [22]:

Part 1 (AB):

$$X = -r_T[1 + \pi \sin\psi / (1 + \cos\psi)] \quad (1)$$

$$Y = -r_T[\pi \cos\psi / (1 + \cos\psi)] \quad (2)$$

Part 2 (BC)

$$X = -r_T(\sin\omega - \cos\omega) \quad (3)$$

$$Y = -r_T(\cos\omega + \sin\omega) \quad (4)$$

Part 3: (C'D):

$$X = r_T(\cos\acute{\omega} + \acute{\omega}\sin\acute{\omega}) \quad (5)$$

$$Y = r_T(\sin\acute{\omega} - \acute{\omega}\cos\acute{\omega}) \quad (6)$$

Part 4 (DA '):

$$X = r_T\pi\cos\acute{\psi}/(1+\cos\acute{\psi}) \quad (7)$$

$$Y = r_T[1 + \pi\sin\acute{\psi}/(1+\cos\acute{\psi})] \quad (8)$$

where: ω: involute concentrator's angle; $\acute{\omega}$: upper involute concentrator's angle; ψ: parabolic concentrator's angle; $\acute{\psi}$: upper parabolic concentrator's angle; $\acute{\psi} = \psi = 58$ degrees and $\omega = \acute{\omega} = 90$ degrees [22].

The width of the concentrator ($W\alpha$) is $AA' = BD = 2\pi r_T$ [22]. As the radius of the storage tank (r_T) was chosen as 15 cm, $W\alpha$ is 95 cm and the length of the aperture (L_α), which is equal to the length of the storage tank (L_T), is 200 cm. This results in the aperture area (A_α) of 16,500 cm^2 for the SWH system. To obtain the exact dimensions of the curves, a computer program was written based on the above equations to calculate the coordinates of the points for each degree of variation of ψ and ω. The system specification is presented in Table 1.

Table 1: Configuration details of the tested ICS SWH

where: D_T : Diameter of the storage tank; V_T: Volume of the storage tank, A_r: area of absorber; CR: concentration ratio.

It should be noted that the concentrator should not oxidize during operation as it will reduce its smoothness. In the market, polished sheets that have high reflection properties include mirrors [13], steel sheets and aluminum foil. Each of the three concentrators was installed on the water heater, and various experiments were carried out to ultimately select the concentrator that had the best thermal performance. The general characteristics of the designed ICS SWH are summarized in Table 2.

Table 2: General characteristics of the water heater

3. Construction and assembly

Based on the results obtained in the previous section, an ICS SWH with a symmetric CPC concentrator was developed (Figs. 3 and 4). The structure of an ICS SWH should be light and portable, and also compatible with local climatic conditions. Therefore, chipboard was selected to build the structure of the SWH. As the system should be thermally insulated, the structure was covered with glass wool. To ensure the water heater's screen was always perpendicular to the incoming sunlight, a manual sun tracker system was placed in the back of the water heater, which was able to adjust the position of the regulator to desired angles (Fig. 4). This allowed to the angle of the water heater to be changed daily, monthly or seasonally, for maximum efficiency. It should be noted that this angle would change with the latitude of the area where it is installed.

Fig. 3 – Construction and assembly of the ICS SWH system

4. Experimental analysis and data collection

4.1. Thermal performance of concentrators

The mean daily efficiency of the system can be determined as [43].

$$\eta_d = Q_W / Q_R \quad (9)$$

where: η_d: mean daily efficiency; Q_W: heat in water storage tank; Q_R: integrated solar radiation on the system aperture. The value of Q_W without any water drainage during the day is determined as:

$$Q_W = M_w C_{p,w}(T_1 - T_0) \quad (10)$$

where: M_w: mass of water; $C_{p,w}$: specific heat of water; T_0: initial storage water temperature; T_1: final storage water temperature.

The total amount of solar radiation entering the aperture area of SWH during the day (from time t0 (7:00) to time t1 (19:00)), is obtained by integrating the intensity field G(t) [44]:

$$Q_R = A_a \int_{t_0}^{t_1} G(t)\ dt \quad (11)$$

$$G_m = (\int_{t_0}^{t_1} G(t)\, dt)/Dt \quad (12)$$

where: G_m : mean daily solar radiation intensity; Dt: time interval during daily operation.

Therefore, the mean daily efficiency can be determined as a function of the ratio DT_{mD}/G_m ($Kw^{-1}m^2$), by second-degree polynomial fitting [45]:

$$\eta_d = C + B(DT_{mD}/G_m) + A\,(DT_{mD}/G_m)^2 \quad (13)$$

where: $DT_{mD} = ((T_0 + T_1)/2) - T_{ma}$; T_{ma}: mean ambient temperature. The coefficient C represents the mean daily efficiency of the system in the case of $(T_0 + T1)/2 = T_{ma}$, and A, B are the thermal loss parameters of the system during the daily operation [46].

For night time operation, the thermal losses of the system are considered to be introduced with the parameter U_s, which expresses the thermal performance of the system from afternoon until the following morning, when the system does not catch any solar radiation**.** The night-time heat loss coefficient (U_s) can be calculated by the following equation [47]:

$$U_s = (\rho C_{p,w} V_T/Dt)\ln[(T_{0m} - T_{am})/(T_{1m} - T_{am})] \quad (14)$$

where: V_T: the volume of storage tank; ρ: density of water; Dt: time interval; T_0: mean initial storage water temperature; T_1: mean final storage water temperature; T_{am}: mean ambient temperature.

Fig. 4: The constructed ICS SWH at the testing site in Kerman

4.2. Measurement apparatus

A k-type thermocouple was used to measure the temperature of the water, Tw, and the ambient temperature, Ta, with accuracy of ± 1.5 °C for temperature range of 0-200 °C. A Kipp and Zonen pyranometer (Model: CMP22) was utilised to measure the radiation input to the collector. The accuracy of the pyranometer was ± 5 W/m². All the data were collected using a data logger (Model: ST-8891E) and a laptop.

4.2. Data collection and error analysis

4.3. Data collection and error analysis

Following the collection of water temperature and solar radiation intensity data, the raw data was converted into meaningful information using relevant graphs to analyze the rate of change and observe the performance of the system in hourly manner. Linear and second-order polynomial functions were fitted to the data of variations of overnight thermal loss coefficients and mean daily efficiency respectively. The error of curve-fitting was determined for each case using coefficient of determination (R^2) and they are presented in Tables 3, 4, 6 and 7.

4.3. Selection and testing of the concentrator

To achieve optimal performance, selecting a proper concentrator has an important effect on the thermal efficiency of the solar system [48]. Experiments were carried out with the installation of different concentrators on the system and the evaluation of their thermal performances. Based on the available material for concentrators in the market, mirror, steel sheet, and aluminum foil were selected. The first experiment was performed by installing the aluminum foil on the system and testing for three consecutive days (see Fig. 5). The water temperature at the start (of all tests) was 21 °C. On the first day of the test, the temperature of the water inside the storage tank reached 43 °C while on the second and third days it reached 53 °C and 61 °C respectively. By replacing the concentrator and installing the steel sheet or mirror, the temperature of the water inside the storage tank increased throughout the day (see Fig. 5).

Fig. 5 - Temperature changes for three consecutive days (M_b: Mirror booster , A_f: Aluminum foil, S_s: Steal sheet, T_a: ambient temperature , G: incoming solar radiation intensity)

Fig. 6 – Overnight thermal loss coefficients and mean daily efficiency (M_b: □, A_f: ○, S_s: ▲)

It can be seen from Fig. 5 that the temperature reduction during the night was the highest for the mirror. The variations of overnight thermal loss coefficients and mean daily efficiency are plotted in Fig. 6. By fitting a second-order polynomial function [49] to the points obtained, an equation for the mean daily efficiency was obtained for each material (Table 3). According to the equations in Table 3, the coefficient C of mean daily efficiency equations was highest (0.667) for the mirror, and it was 0.476 for the steel sheet and 0.437 for the aluminum foil. This indicates that the output of the mirror was better than the steel sheet and aluminum foil during the day.

Table 3. Equations of mean daily efficiency of concentrators

In the same way, a first-order line [49] was fitted for the obtained points of the thermal loss coefficient, and the equations for the 3 concentrators are shown in Table 4. The main part of equation [43] is 6.9877 for the aluminum foil, 8.0035 for the steel sheet and 11.016 for the mirror. The results indicate that, although the steel sheet has the second highest efficiency among the experimented materials, it has an acceptable heat loss in compression with the mirror. In addition, it is cheaper and easy to install [24]. Therefore, the steel sheet was selected in the ICS SWH system for monthly experiments (see Fig. 6).

Table 4. Equations of overnight thermal loss coefficient (U_s) for different concentrators

4.4. Thermal performance of the ICS SWH in 6 different months in Kerman

Since the solar slope angle changes every month, the angle of the ICS SWH needs to be adjusted to obtain maximum solar radiation. Table 5 provides the optimal angles for obtaining the highest solar radiation for some Iranian cities [50]. According to this table, for Kerman, the optimal angle.

Table 5 - The solar slope angles in degree (°) at different months for 6 cities in Iran [50]

changes by about 7 to 8 degrees in every month. For each month, the data of the temperature changes (the ambient temperature and temperature of the water in the storage tank) and the amount of radiation entering the system for three consecutive days were collected and the results are plotted in Fig. 7. Then, using equations (13) and (14), the mean daily efficiency and overnight thermal loss coefficients were determined at different time intervals and the results are plotted in Fig. 8. The equations of mean daily efficiency and overnight thermal loss coefficient by fitting the obtained points are evaluated for 6 different months (see Tables 6 & 7).

Table 6: The system's mean daily efficiency (η_d) in different months in Kerman

Table 7: Overnight heat loss coefficient of the system (U_s) in different months in Kerman

The first monthly test was carried out in April and according to Table 4, the ICS SWH was adjusted with solar slope angle (β=14.55°). The water temperature was 21 °C at the start of the test and the temperature of the water reached 65 °C on the third day of the experiment. The recorded temperature changes in April are presented in Fig. 7.

Fig. 7 – Tw, Ta and G for three consecutive days in 6 different months

By using the efficiency equation, the coefficients C, B, and A were determined and shown in Fig. 8. The coefficient C is defined as the maximum efficiency of the ICS SWH system, which according to the results obtained, is 0.6557. Similarly, considering Equation 14, the heat loss coefficient of ICS SWH was obtained during the night (see Fig. 8).

Fig. 8 – Mean daily efficiency (left) and heat loss coefficient (right) of ICS SHW in Kerman (6 mounts)

In May, with the warming of the climate and changing angle of the sun, according to Table 4 for Kerman (β was set to 77.1 °), the ICS SHW system was tested. The pyranometer recorded a solar radiation intensity of 980 W/m^2 in May. The water temperature in the storage tank reached 72 C^o.

Fig. 7 shows the temperature changes for three consecutive days. The mean daily efficiency and heat loss coefficient graphs are presented in Fig. 8, and the relevant equations are listed in Tables 6 and 7. The coefficient C for May is 0.6129, which is less than the value in April.

The third test was conducted in June at a slope angle of -4.89 ° (slope to the North). The temperature changes on three consecutive days are shown in Fig. 7. The maximum temperature of the water was measured as 73 °C, which was more than for the three days of the experiments in April and May.

For testing in July, the water heater angle was set to -2.8 °. The maximum solar radiation intensity that the pyranometer displayed was 1120 W/m^2. The temperature of the water after three days of testing reached 74 °C, and the difference between the water temperature at the start and end of the test was 52 °C, which was the highest difference compared to the earlier recorded months. Looking at the coefficient C in the equations (Table 7), the test carried out in July has the smallest amount of heat loss. To evaluate the thermal performance of the system in August, the acceptance angle of the system (α) was adjusted to 83.93°. The sun's radiation intensity declined in comparison with July, and hence, this month can be considered as a turning point in terms of solar radiation. Mean daily performance also rose in August, whereas it had gone down in the previous months, which can also be considered as a turning point in the ICS SWH. The last test was carried out in September at an angle of β=26.63°. The highest temperature changes for the first, second and third days of the experiment were 31 °C, 13.5 °C, and 21 °C respectively. In September, the coefficient C and the efficiency of the water heater increased (See Fig. 9).

Fig. 9 – Thermal efficiency of the ICS SWH and mean daily radiation in 6 different months in Kerman, Iran

5. Conclusion

This paper presented the design, fabrication and testing of an ICS SWH system for Kerman in Iran. The developed ICS SWH can be used to heat water in houses or preheat water in small to medium-sized industries. The main advantages of this system, compared with the available models on the market, are inexpensive materials and portability. The developed system provides an alternative solution for heating water, especially in remote rural areas.

The tested ICS SWH showed acceptable efficiency in comparison with similar systems [40]. Looking at the changes in coefficient C (Table 6), it can be noted that by increasing the amount of radiation entering the water heater, the thermal efficiency of the system decreases, such that the highest efficiency was in April and the lowest was in July. With the distribution of radiation intensity in the months of August and September, the thermal efficiency of the system increased. Based on these results, the highest efficiency would be in the colder months or in colder regions. This is in agreement with the results reported in [51].

By increasing solar radiation intensity, the capacity of energy absorption of the system decreased, since a temperature gradient rise will increase the heat loss due to convective heat transfer and radiation [52]. Also, the results shows that by increasing the temperature of the water in the storage tank, the radiated heat loss from the system increases.

One of the influential parameters on the system's performance is the temperature gradient between the ambient air and water inside the storage tank. The results of this study showed that by increasing the ambient temperature in hot climatic conditions such as those of Kerman, the radiated energy potential in the system decreases. Therefore, constant withdrawal of hot water from the tank can be recommended to help increase efficiency.

The results of the experiments with the three common concentrators – mirror booster, steel sheet and aluminum foil – showed that using mirror reflection can increase the thermal efficiency of the system, but on the other hand, can lead to more thermal losses in the system. The steel sheet is the optimal amongst the materials tested, as it is economically affordable, stronger and also easy to install in rural areas in Kerman.

Funding

None.

Declaration of Competing Interest

None declared.

Acknowledgement

The authors would like to appreciate the anonymous reviewers for their insightful comments and suggestions.

References

1. Quaschning, V.V., *Renewable Energy and Climate Change, 2nd Edition*. 2019: Wiley.
2. Khare, V., S. Nema, and P. Baredar, *Solar–wind hybrid renewable energy system: A review.* Renewable and Sustainable Energy Reviews, 2016. 58: p. 23-33.

3. Alotaibi, D.M., M. Akrami, M. Dibaj, and A.A. Javadi, *Smart energy solution for an optimised sustainable hospital in the green city of NEOM.* Sustainable Energy Technologies and Assessments, 2019. 35: p. 32-40.
4. de Freitas Viscondi, G. and S.N. Alves-Souza, *A Systematic Literature Review on big data for solar photovoltaic electricity generation forecasting.* Sustainable Energy Technologies and Assessments, 2019. 31: p. 54-63.
5. Sow, A., M. Mehrtash, D.R. Rousse, and D. Haillot, *Economic analysis of residential solar photovoltaic electricity production in Canada.* Sustainable Energy Technologies and Assessments, 2019. 33: p. 83-94.
6. Chilundo, R.J., D. Neves, and U.S. Mahanjane, *Photovoltaic water pumping systems for horticultural crops irrigation: Advancements and opportunities towards a green energy strategy for Mozambique.* Sustainable Energy Technologies and Assessments, 2019. 33: p. 61-68.
7. Garcia, A.G., N. Sras, and M. Zuhir, *Energy Resources Analysis.* 2017.
8. Patel, K., P. Patel, and J. Patel, *Review of solar water heating systems.* International Journal of Advanced Engineering Technology, 2012. 3(4): p. 146-149.
9. Hohne, P., K. Kusakana, and B. Numbi, *A review of water heating technologies: An application to the South African context.* Energy Reports, 2019. 5: p. 1-19.
10. Shukla, R., K. Sumathy, P. Erickson, and J. Gong, *Recent advances in the solar water heating systems: A review.* Renewable and Sustainable Energy Reviews, 2013. 19: p. 173-190.
11. Chan, H.-Y., S.B. Riffat, and J. Zhu, *Review of passive solar heating and cooling technologies.* Renewable and Sustainable Energy Reviews, 2010. 14(2): p. 781-789.
12. Gautam, A., S. Chamoli, A. Kumar, and S. Singh, *A review on technical improvements, economic feasibility and world scenario of solar water heating system.* Renewable and Sustainable Energy Reviews, 2017. 68: p. 541-562.
13. Jamali, H., *Investigation and review of mirrors reflectance in parabolic trough solar collectors (PTSCs).* Energy Reports, 2019. 5: p. 145-158.
14. Jamar, A., Z. Majid, W. Azmi, M. Norhafana, and A. Razak, *A review of water heating system for solar energy applications.* International Communications in Heat and Mass Transfer, 2016. 76: p. 178-187.

15. Fernández-García, A., E. Zarza, L. Valenzuela, and M. Pérez, *Parabolic-trough solar collectors and their applications.* Renewable and Sustainable Energy Reviews, 2010. 14(7): p. 1695-1721.

16. Tiller, J. and V. Wochatz. *Performance of integrated passive solar water heaters (Breadbox-type) under varying design conditions in the South-eastern US*. in *Proceedings of the Seventh National Passive Solar Conference, Knoxville, TN, USA*. 1982.

17. Garg, H., G. Datta, and A. Bhargava, *Studies on an all plastic solar hot water bag.* International journal of energy research, 1984. 8(3): p. 291-296.

18. Faiman, D., *Towards a standard method for determining the efficiency of integrated collector-storage solar water heaters.* Solar energy, 1984. 33(5): p. 459-463.

19. Weller, P., G. Clark, and W. Collins. *Indoor testing of an integral passive solar water heater*. in *Proceedings of the 10th national passive solar conference*. 1985.

20. Rommel, M. and A. Wagner, *Application of transparent insulation materials in improved flat-plate collectors and integrated collector storages.* Solar energy, 1992. 49(5): p. 371-380.

21. Mohamad, A., *Integrated solar collector–storage tank system with thermal diode.* Solar Energy, 1997. 61(3): p. 211-218.

22. Tripanagnostopoulos, Y. and M. Souliotis, *Integrated collector storage solar systems with asymmetric CPC reflectors.* Renewable Energy, 2004. 29(2): p. 223-248.

23. M. Smyth , P.C.E., B. Norton, *Evaluation of a freeze resistant integrated collector/storage solar water-heater for northern Europe.* Applied Energy, 2001. 68: p. 265-274.

24. Smyth, M., P. Eames, and B. Norton, *Techno-economic appraisal of an integrated collector/storage solar water heater.* Renewable Energy, 2004. 29(9): p. 1503-1514.

25. Souliotis, M. and Y. Tripanagnostopoulos, *Experimental study of CPC type ICS solar systems.* Solar Energy, 2004. 76(4): p. 389-408.

26. Assari, M.R., H.B. Tabrizi, and M. Savadkohy, *Numerical and experimental study of inlet-outlet locations effect in horizontal storage tank of solar water heater.* Sustainable Energy Technologies and Assessments, 2018. 25: p. 181-190.

27. Souliotis, M. and Y. Tripanagnostopoulos, *Study of the distribution of the absorbed solar radiation on the performance of a CPC-type ICS water heater.* Renewable Energy, 2008. 33(5): p. 846-858.

28. Benrejeb, R., O. Helal, and B. Chaouachi, *Optical and thermal performances improvement of an ICS solar water heater system.* Solar Energy, 2015. 112: p. 108-119.
29. Benrejeb, R., O. Helal, and B. Chaouachi, *Optimization of the geometrical characteristics of an ICS solar water heater system using the two-level experience planning.* Applied Thermal Engineering, 2016. 103: p. 1427-1440.
30. Harmim, A., M. Boukar, M. Amar, and A. Haida, *Simulation and experimentation of an integrated collector storage solar water heater designed for integration into building facade.* Energy, 2019. 166: p. 59-71.
31. Clifford, M. and D. Eastwood, *Design of a novel passive solar tracker.* Solar Energy, 2004. 77(3): p. 269-280.
32. Nejad, R.M., *A survey on performance of photovoltaic systems in Iran.* Iranica Journal of Energy & Environment, 2015. 6(2): p. 77-85.
33. Rahimzadeh, F., M. Pedram, and M.C. Kruk, *An examination of the trends in sunshine hours over Iran.* Meteorological Applications, 2014. 21(2): p. 309-315.
34. Enjavi-Arsanjani, M., K. Hirbodi, and M. Yaghoubi, *Solar energy potential and performance assessment of CSP plants in different areas of Iran.* Energy Procedia, 2015. 69: p. 2039-2048.
35. Ghorashi, A.H. and A. Rahimi, *Renewable and non-renewable energy status in Iran: Art of know-how and technology-gaps.* Renewable and Sustainable Energy Reviews, 2011. 15(1): p. 729-736.
36. Heidari, H., S.T. Katircioglu, and L. Saeidpour, *Natural gas consumption and economic growth: Are we ready to natural gas price liberalization in Iran?* Energy Policy, 2013. 63: p. 638-645.
37. Hamid, B., A. Mohammad Bagher, B. Mohammad Reza, and B. Mahboubeh, *Review of sustainable energy sources in Kerman.* World Journal of Engineering, 2016. 13(2): p. 109-119.
38. Roya, N. and B. Abbas, *Colorectal cancer trends in Kerman province, the largest province in Iran, with forecasting until 2016.* Asian Pacific Journal of Cancer Prevention, 2013. 14(2): p. 791-793.

39. Besarati, S.M., R.V. Padilla, D.Y. Goswami, and E. Stefanakos, *The potential of harnessing solar radiation in Iran: Generating solar maps and viability study of PV power plants.* Renewable energy, 2013. 53: p. 193-199.

40. Smyth, M., P. Eames, and B. Norton, *Integrated collector storage solar water heaters.* Renewable and Sustainable Energy Reviews, 2006. 10(6): p. 503-538.

41. Keshavarzi, A., M. Sharifzadeh, A.K. Haghighi, S. Amin, S. Keshtkar, and A. Bamdad, *Rural domestic water consumption behavior: A case study in Ramjerd area, Fars province, IR Iran.* Water research, 2006. 40(6): p. 1173-1178.

42. Kenisarin, M. and K. Mahkamov, *Solar energy storage using phase change materials.* Renewable and sustainable energy reviews, 2007. 11(9): p. 1913-1965.

43. Souliotis, M., S. Kalogirou, and Y. Tripanagnostopoulos, *Modelling of an ICS solar water heater using artificial neural networks and TRNSYS.* Renewable Energy, 2009. 34(5): p. 1333-1339.

44. Helal, O., B. Chaouachi, and S. Gabsi, *Design and thermal performance of an ICS solar water heater based on three parabolic sections.* Solar Energy, 2011. 85(10): p. 2421-2432.

45. Tripanagnostopoulos, Y. and M. Souliotis, *ICS solar systems with two water tanks.* Renewable Energy, 2006. 31(11): p. 1698-1717.

46. Tripanagnostopoulos, Y. and M. Souliotis, *ICS solar systems with horizontal (E–W) and vertical (N–S) cylindrical water storage tank.* Renewable Energy, 2004. 29(1): p. 73-96.

47. Tripanagnostopoulos, Y. and M. Souliotis, *ICS solar systems with horizontal cylindrical storage tank and reflector of CPC or involute geometry.* Renewable Energy, 2004. 29(1): p. 13-38.

48. Harris, J.A. and T.G. Lenz, *Thermal performance of solar concentrator/cavity receiver systems.* Solar energy, 1985. 34(2): p. 135-142.

49. Garnier, C., T. Muneer, and J. Currie, *Numerical and empirical evaluation of a novel building integrated collector storage solar water heater.* Renewable energy, 2018. 126: p. 281-295.

50. Talebizadeh, P., M. Mehrabian, and M. Abdolzadeh, *Determination of optimum slope angles of solar collectors based on new correlations.* Energy Sources, Part A: Recovery, Utilization, and Environmental Effects, 2011. 33(17): p. 1567-1580.

51. Dieng, A. and R. Wang, *Literature review on solar adsorption technologies for ice-making and air-conditioning purposes and recent developments in solar technology.* Renewable and sustainable energy reviews, 2001. 5(4): p. 313-342.

52. Kumar, R. and M.A. Rosen, *Thermal performance of integrated collector storage solar water heater with corrugated absorber surface.* Applied Thermal Engineering, 2010. 30(13): p. 1764-1768.

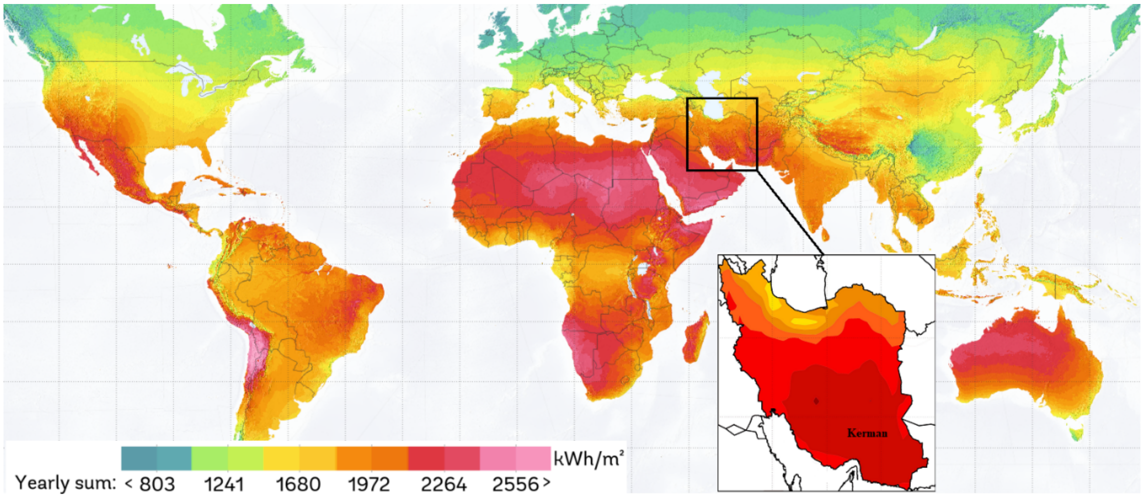

Fig. 1: Comparing Annual solar radiance of Kerman with the rest of the world (kWh/m) [39].

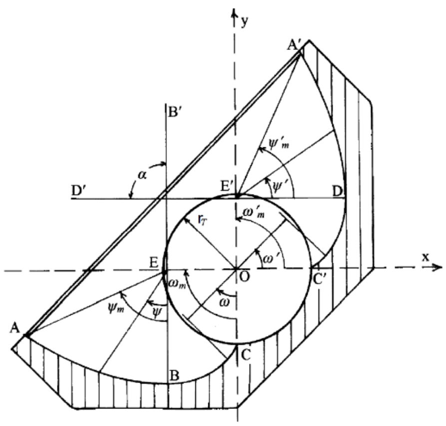

Fig. 2: Cross-section view of a symmetric CPC [22]

Fig. 3: Construction and assembling the ICS SWH system

Fig. 4: The constructed ICS SWH at the testing site in Kerman

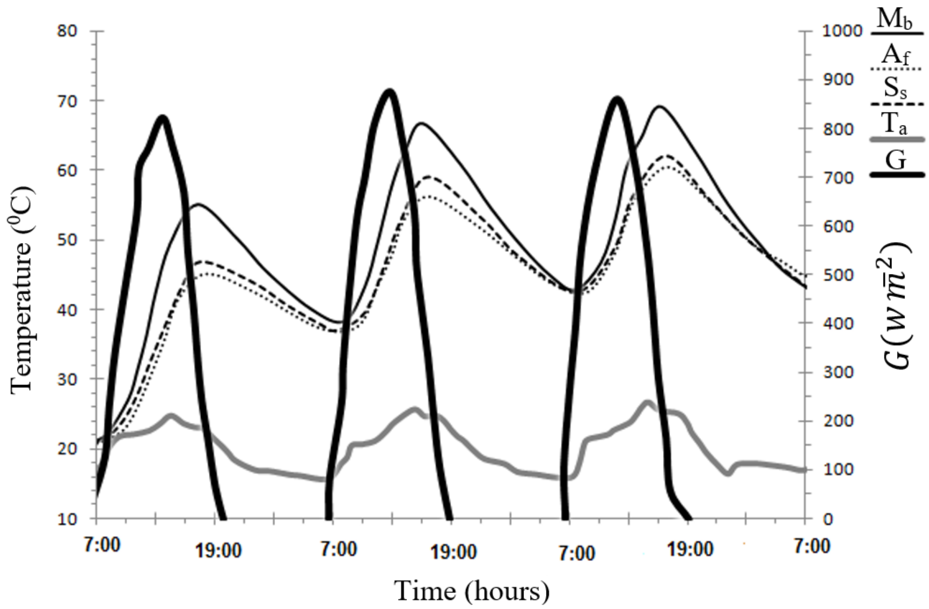

Fig. 5 - Temperature changes for three consecutive days (M_b: Mirror booster , A_f: Aluminum foil, S_s: Steal sheet, T_a: ambient temperature , G: incoming solar radiation intensity)

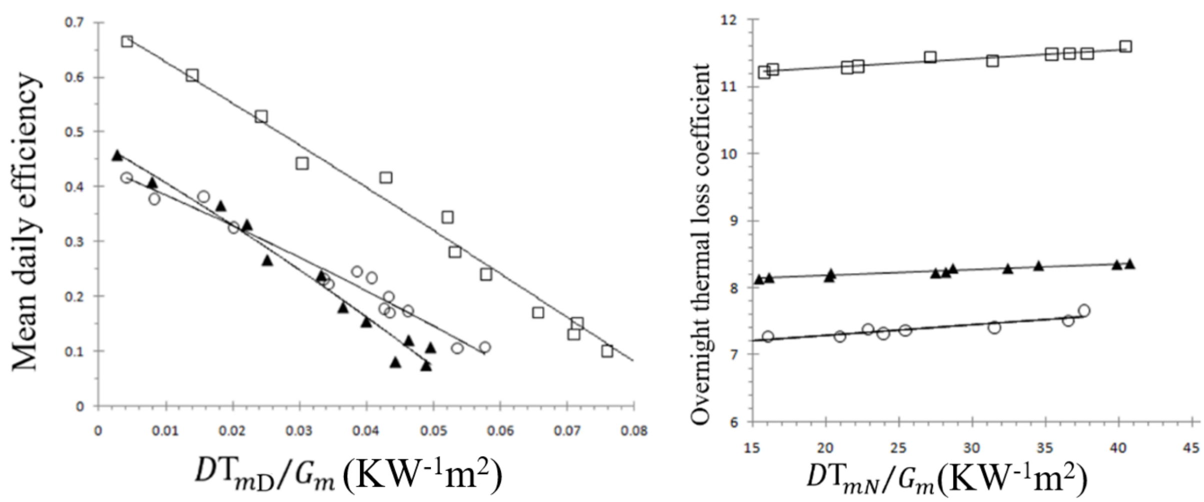

Fig. 6 – Overnight thermal loss coefficients and mean daily efficiency (M_b: □, A_f: ○, S_s: ▲)

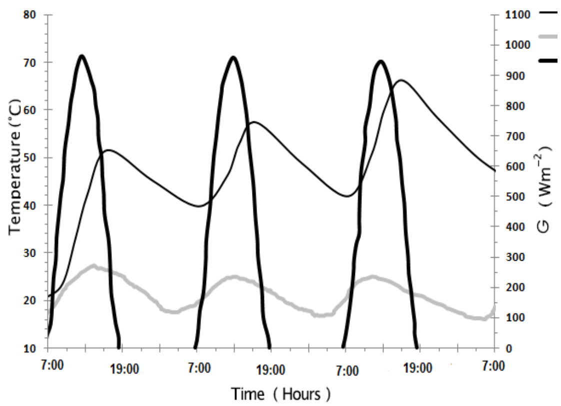

April

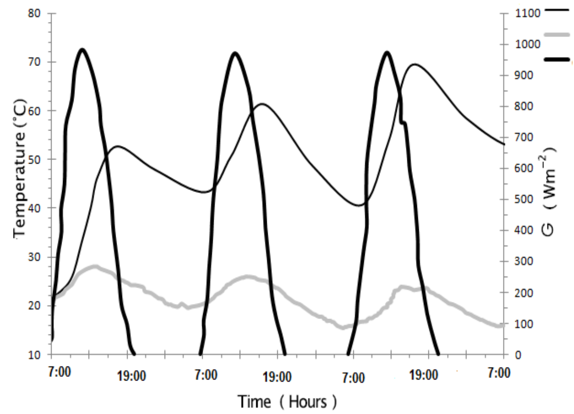

May

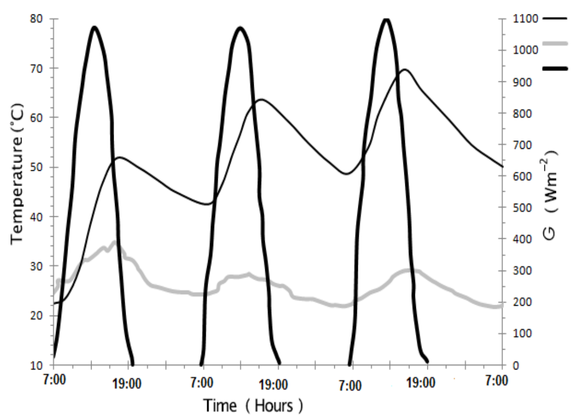

June

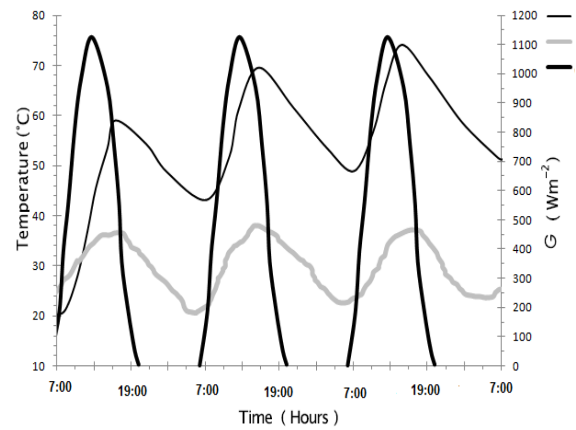

July

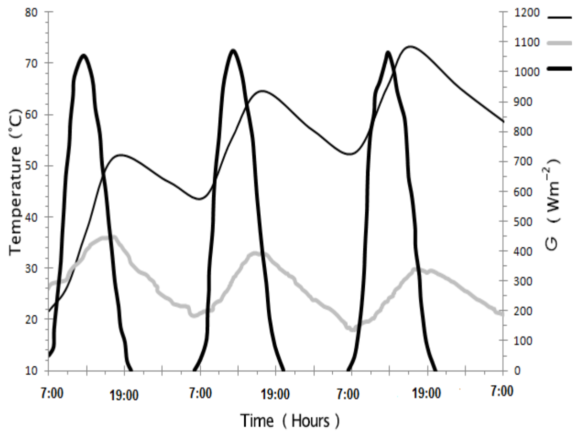

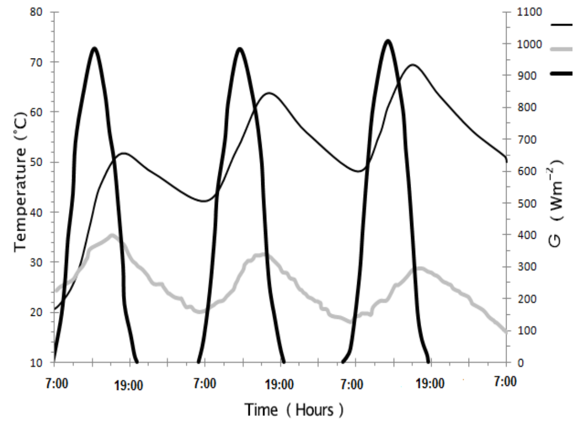

August

September

Fig. 7 – Tw, Ta and G for three consecutive days in 6 different months

637

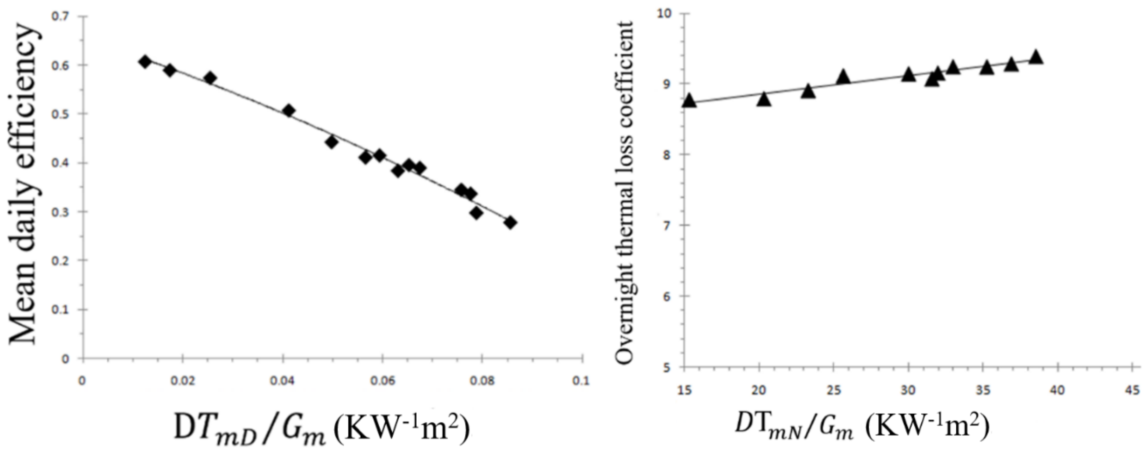
Mean daily efficiency
0.7
0.6
0.5
0.4
0.3
0.2
0.1
0
0
0.02
0.04
0.06
0.08
0.1
DT_{mD}/G_m (KW-1m2)
Overnight thermal loss coefficient
10
9
8
7
6
5
15
20
25
30
35
40
45
DT_{mN}/G_m (KW-1m2)

April

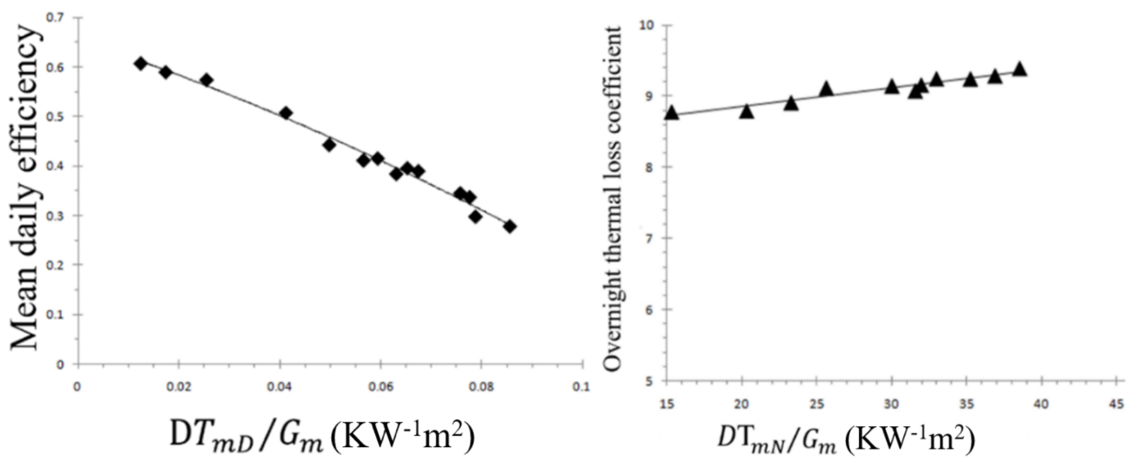
Mean daily efficiency
0.7
0.6
0.5
0.4
0.3
0.2
0.1
0
0
0.02
0.04
0.06
0.08
0.1
DT_{mD}/G_m (KW-1m2)
Overnight thermal loss coefficient
10
9
8
7
6
5
15
20
25
30
35
40
45
DT_{mN}/G_m (KW-1m2)

May

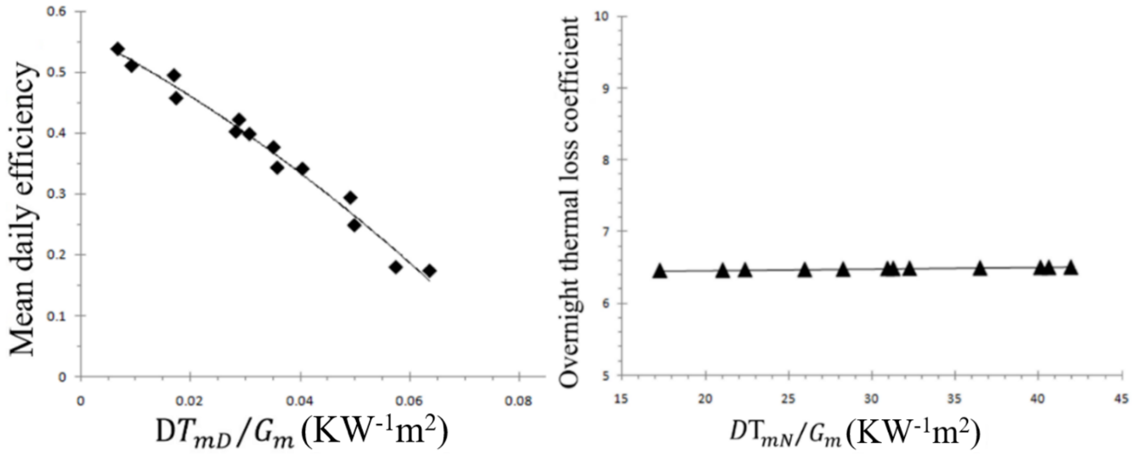
Mean daily efficiency
DT_{mD}/G_m (KW-1m2)
Overnight thermal loss coefficient
DT_{mN}/G_m (KW-1m2)

June

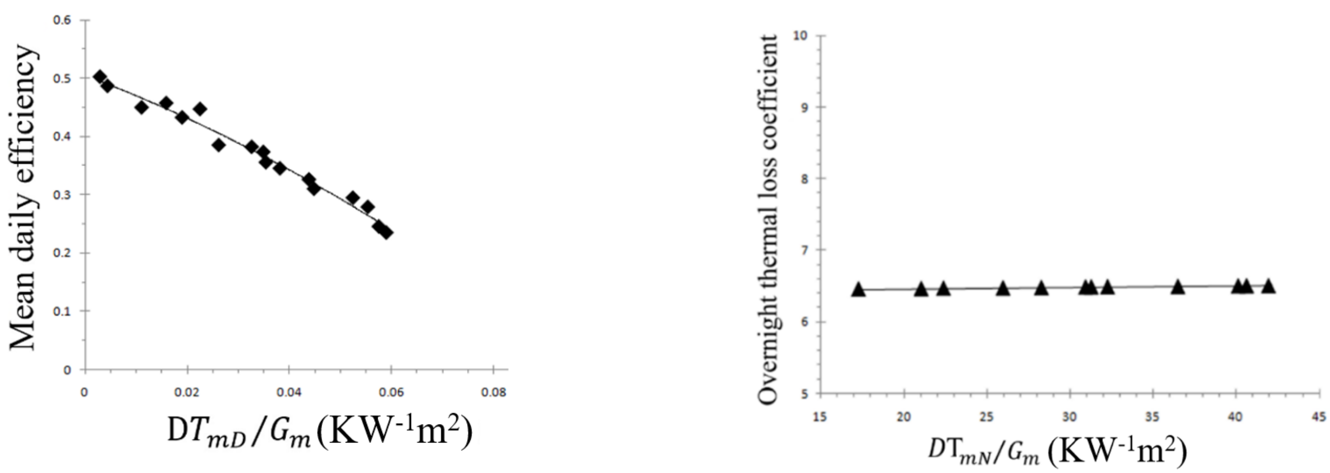
Mean daily efficiency
DT_{mD}/G_m (KW-1m2)
Overnight thermal loss coefficient
DT_{mN}/G_m (KW-1m2)

July

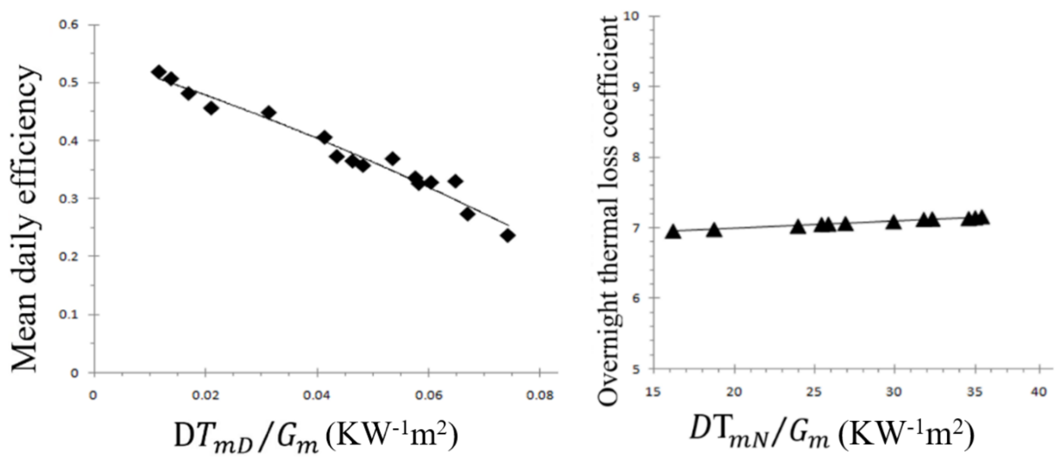

August

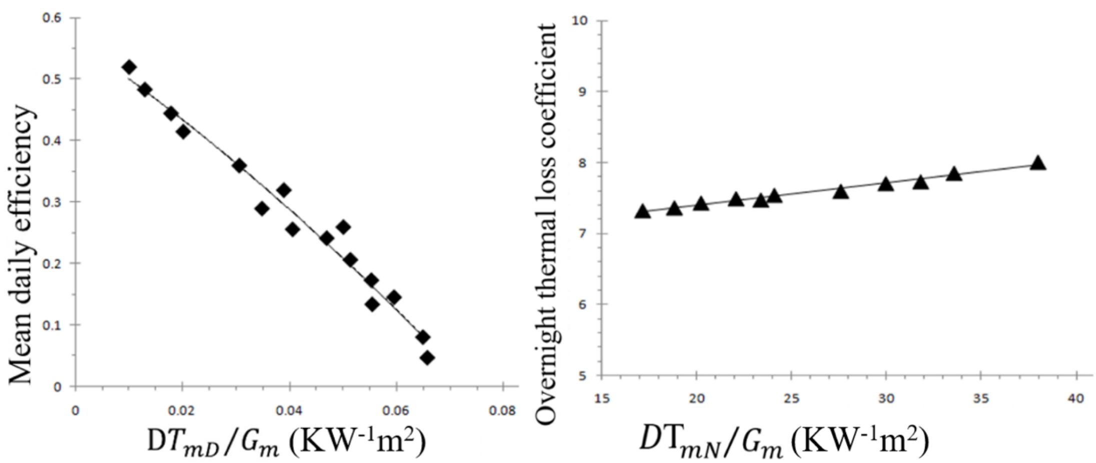

September

Fig. 8 – Mean daily efficiency (left) and heat loss coefficient (right) of ICS SHW in Kerman (6 mounts)

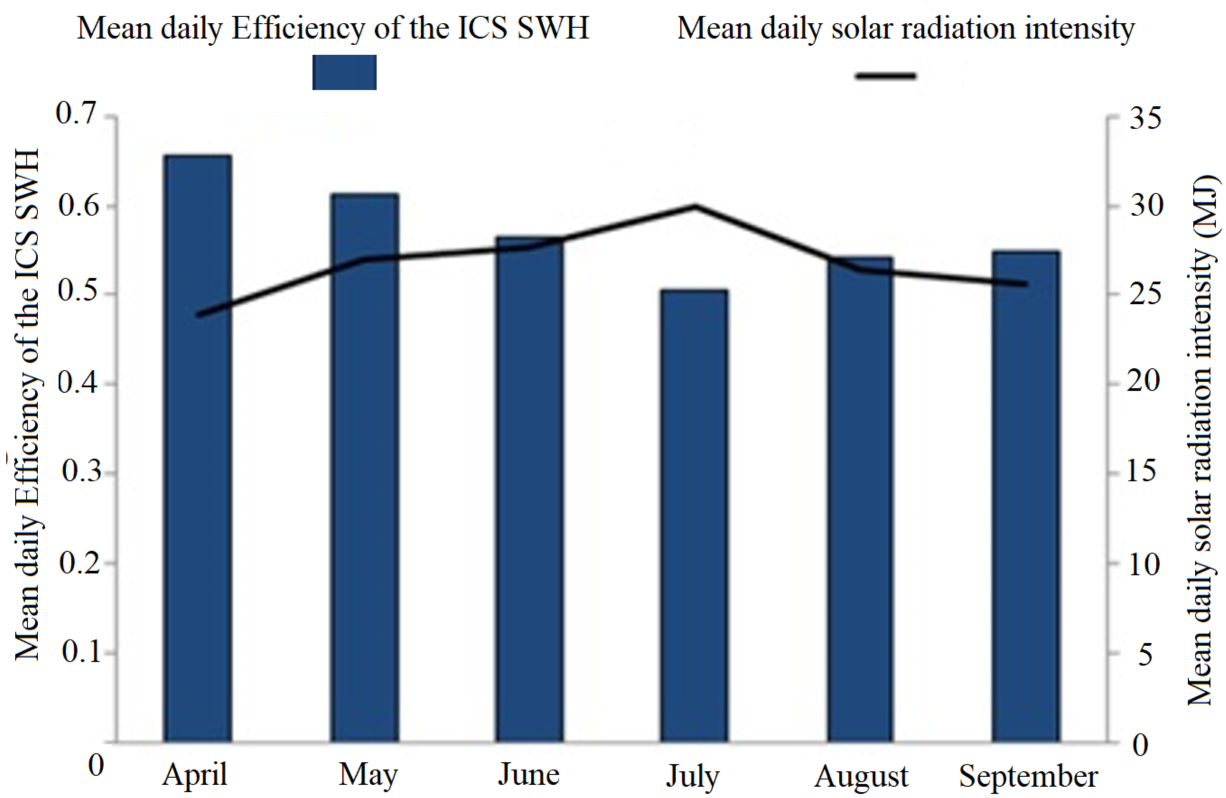

Fig. 9 – Thermal efficiency of the ICS SWH and mean daily radiation in 6 different months in Kerman, Iran

Table 1: Configuration details of the tested ICS SWH

D_T	V_T	W_α	A_α	A_r	$\frac{V_T}{A_\alpha}$	CR
30 cm	140 liter	82 cm	16500 cm^2	14100 cm^2	84/64	1/17

Table 2 : General characteristics of the water heater

Complete system	Dimension	200×64×113 cm
	Aperture area of systems	1.89 m^2
	Material of aperture	Simple flute glass
Concentrator	Kind of concentrator	CPC
	Material of concentrator	Steel sheet, aluminum foil, and mirror booster
Storage tank	Capacity	140 liters
	Material	Galvanized sheet
	Insulating material	Black enamel

Table 3. Equations of mean daily efficiency of concentrators

Material	Mean daily efficiency equation η_d	Coefficient of determination
Mirror booster	$\eta_d = 0.667 - 7.4215(DT_{mD}/G_m) - 4.418(DT_{mD}/G_m)^2$	$R^2 = 0.9443$
Steel sheet	$\eta_d = 0.5262 - 8.2903(DT_{mD}/G_m) - 11.561(DT_{mD}/G_m)^2$	$R^2 = 0.9490$
Aluminum foil	$\eta_d = 0.4872 - 5.128(DT_{mD}/G_m) - 14.072(DT_{mD}/G_m)^2$	$R^2 = 0.9574$

Table 4: Equations of overnight thermal loss coefficient (U_s) for different concentrators

Material	Mean daily efficiency equation η_d	Coefficient of determination
Mirror booster	U_s =11.016+ 0.0132(DT_{mN}/G_m)	R^2 = 0.8081
Steel sheet	U_s =8.0035+0.009(DT_{mN}/G_m)	R^2 = 0.8742
Aluminum foil	U_s =6.9877 +0.0153(DT_{mN}/G_m)	R^2 = 0.7789

Table 5 - The solar slope angles in degree (°) at different months for 6 cities in Iran [50]

Month	Zahedan	Birjand	Shiraz	Tabas	Yazd	Kerman
January	54.14	58.37	54.64	57.69	56.72	52.83
February	44.00	47.60	40.48	47.82	47.59	2.31
March	30.01	33.28	26.22	33.07	32.50	27.83
April	14.71	17.25	13.34	17.87	16.65	14.55
May	0.97	3.89	1.31	4.68	2.98	1.77
June	-5.28	-2.80	-5.23	-1.94	-3.91	-4.89
July	-2.74	-0.10	-2.07	0.88	-0.97	-2.08
August	9.02	12.24	8.79	12.65	11.32	9.83
September	25.53	28.92	24.96	28.80	28.21	26.63
October	40.64	43.66	39.57	44.32	44.04	41.76
November	52.75	55.92	51.01	55.97	54.72	54.67
December	56.62	60.94	57.50	60.15	58.80	58.62

Table 6: The system's mean daily efficiency (η_d) in different months in Kerman

Months	Mean daily efficiency equation η_d	Coefficient of determination
April	$\eta_d = 0.6557 - 3.3923(DT_{mD}/G_m) - 11.483(Dt_{mD}/G_m)^2$	$R^2 = 0.9760$
May	$\eta_d = 0.6129 - 4.4034(DT_{mD}/G_m) - 6.1728(DT_{mD}/G_m)^2$	$R^2 = 0.9712$
June	$\eta_d = 0.5647 - 4.6561(DT_{mD}/G_m) - 27.468(DT_{mD}/G_m)^2$	$R^2 = 0.9585$
July	$\eta_d = 0.5046 - 3.3051(DT_{mD}/G_m) - 18.606(DT_{mD}/G_m)^2$	$R^2 = 0.9643$
August	$\eta_d = 0.5429 - 2.9902(DT_{mD}/G_m) - 12.211(DT_{mD}/G_m)^2$	$R^2 = 0.9206$
September	$\eta_d = 0.5525 - 5.9753(DT_{mD}/G_m) - 22.128(DT_{mD}/G_m)^2$	$R^2 = 0.9663$

Table 7: Overnight heat loss coefficient of the system (U_s) in different months in Kerman

Months	Mean daily efficiency equation η_d	Coefficient of determination
April	$U_s = 8.3357 + 0.0261(DT_{mN}/G_m)$	$R^2 = 0.9648$
May	$U_s = 7.1134 + 0.0223(DT_{mN}/G_m)$	$R^2 = 0.9444$
June	$U_s = 6.4208 + 0.0019(DT_{mN}/G_m)$	$R^2 = 0.8447$
July	$U_s = 5.7184 + 0.0152(DT_{mN}/G_m)$	$R^2 = 0.9259$
August	$U_s = 6.7821 + 0.0102(DT_{mN}/G_m)$	$R^2 = 0.8542$
September	$U_s = 6.79 + 0.0315(DT_{mN}/G_m)$	$R^2 = 0.9677$

Abbreviation

D_T	Diameter of storage tank (cm)	A_α	Area of aperture (cm^2)
V_T	Volume of storage tank (liter)	A_r	Area of absorber (cm^2)
CR	Concentration Ratio	C	Maximum mean daily efficiency coefficient
ICS	Integrated collector storage	Q_W	Heat in the tank of water storage (J)
SWH	Solar water heater	Q_R	Integrated solar radiation on the aperture of the system (J)
η_d	Mean daily efficiency	T_{mN}	Mean water temperature difference during the night
r_T	Radius of storage tank	A	Acceptance angle of the system (°, rad)
DT_{mD}	Mean water temperature difference during the day	Dt_D	Time interval during daily operation
CPC	Compound-parabolic-concentrator	T_a	Ambient temperature
W_α	Width of concentrator	G	Incoming solar radiation intensity
L_T	Length of storage tank	D_t	Time interval
L_α	Length of aperture	U_s	Coefficient of thermal losses during the night
M_w	Mass of water	G_m	Mean daily solar radiation intensity
$C_{p,w}$	Specific heat of water	T_0	Initial storage water temperature
A_f	Aluminum foil	t_0	Initial time
T_1	Final storage water temperature	t_1	Final time
T_{ma}	Average ambient temperature	S_S	Steel sheet
M_b	Mirror booster	DT_{mN}	Mean water temperature difference during the night
ω	Involute concentrator's angle (°, rad)	Ψ	Parabolic concentrator's angle (°, rad)
ώ	Upper involute concentrator's angle (°, rad)	ψ́	Upper parabolic concentrator's angle (°, rad)

766

Conflict of interest: None